Design and use of multisine signals for Li-ion battery equivalent circuit modelling. Part 1: Signal design

W.D. Widanage[a,*], A. Barai[a], G. H. Chouchelamane[b], K. Uddin[a], A. McGordon[a], J. Marco[a], P. Jennings[a]

[a] *WMG, University of Warwick, Coventry. CV4 7AL. U.K.*
[b] *Jaguar Land Rover, Banbury Road, Warwick. CV35 0XJ. U.K.*

Abstract

The Pulse Power Current (PPC) profile is often the signal of choice for obtaining the parameters of a Lithium-ion (Li-ion) battery Equivalent Circuit Model (ECM). Subsequently, a drive-cycle current profile is used as a validation signal. Such a profile, in contrast to a PPC, is more dynamic in both the amplitude and frequency bandwidth. Modelling errors can occur when using PPC data for parametrisation since the model is optimised over a narrower bandwidth than the validation profile. A signal more representative of a drive-cycle, while maintaining a degree of generality, is needed to reduce such modelling errors.

In Part 1 of this 2-part paper a signal design technique defined as a pulse-multisine is presented. This superimposes a signal known as a multisine to a discharge, rest and charge base signal to achieve a profile more dynamic in amplitude and frequency bandwidth, and thus more similar to a drive-cycle.

*Corresponding author. Email: Dhammika.Widanalage@warwick.ac.uk. Address: WMG, University of Warwick, Coventry, CV4 7AL, UK. Telephone: 0044 24765 28191.

The signal improves modelling accuracy and reduces the experimentation time, per state-of-charge (SoC) and temperature, to several minutes compared to several hours for an PPC experiment.
Keywords: Multisine signal, Drive-cycle, Li-ion battery, Equivalent Circuit Modelling

---

Abbreviations

DFT Discrete Fourier Transform

ECM Equivalent Circuit Model

NCA Nickel Cobalt Aluminium oxide

NL-ECM Non-linear Equivalent Circuit Model

OCV Open Circuit Voltage

pk-error Peak error

PPC Pulse Power Characterisation

RMSE Root Mean Square Error

SoC State-of-Charge

Notations

A_k : Amplitude of the k^{th} multisine harmonic

α : Scale factor for smallest base-signal pulse $0 < \alpha < 1$

C_1 : C-rate of largest pulse in the base-signal

C_2 : C-rate of smallest pulse in the base-signal

C_{cmax} : Maximum applicable 10 s charge C-rate

C_{dmax} : Maximum applicable 10 s discharge C-rate

F : Highest excited multisine or pulse-multisine harmonic number

f_{max} : Highest desired pulse-multisine frequency (Hz)

f_s : Sampling frequency (Hz)

γ : Scale factor for largest base-signal pulse $0 < \gamma < 1$

H_{exc} : Set of excited multisine harmonics

K : Maximum magnitude of a random-phase multisine signal

N : Number of samples per period of the multisine signal

ϕ_k : Phase of the k^{th} multisine harmonic (rad)

T : Period length of a base-signal, multisine or pulse-multisine (s)

T_1 : Time duration of the larger base-signal pulse (s)

T_2 : Time duration of first rest interval in the base-signal (s)

T_3 : Time duration of the smaller base-signal pulse (s)

T_4 : Time duration of the last rest interval in the base-signal (s)

1. Introduction

The ISO 12405-1/2 and IEC 62660-1/2 documents describe standardised test procedures to evaluate the energy and power performance of Lithium-ion (Li-ion) batteries and packs [1]. The Pulse Power Characterisation (PPC) test is a standardised procedure designed to evaluate the discharge and regenerative power capabilities of a Li-ion battery to varying pulse lengths, currents, state-of-charge (SoC) and battery temperature. The PPC test is a series of alternating 10 s discharge and charge current pulses of increasing C-rate applied at a pre-defined SoC and temperature with a 30 minute rest-interval between each pulse to allow the voltage to relax (Figure 1a). The pulse sequence in Figure 1a is an example used to characterise a cylindrical 3.03 Ah $LiNiCoAlO_2$ (NCA) positive electrode and carbon graphite negative electrode Li-ion battery (1 C$\equiv$ 3.03 A).

From a characterisation perspective the PPC test is designed to be symmetric and as such no net charge or discharge occurs by the end of the pulse sequence. As charge and discharge pulses of increasing currents are used the voltage rise/drop at the end of the 10 second pulse can be plotted with respect to each current pulse and if the plot appears linear the battery dynamics can be considered to behave linearly within that current range.

From a modelling perspective, the voltage response to each 10 s charge

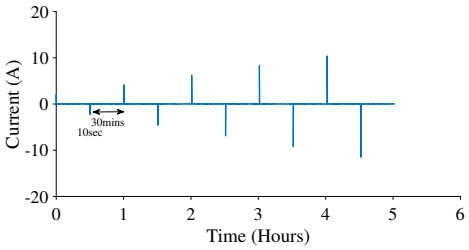

(a) A PPC test sequence example from IEC 62660-1/2 for ECM parameter estimation.

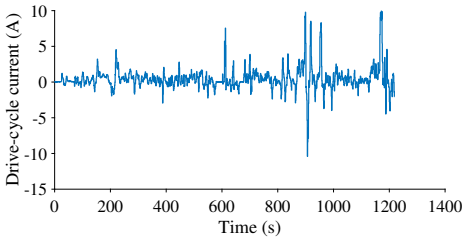

(b) A drive-cycle current profile for ECM validation. Obtained from a prototype EV driving in an urban environment, scaled to a 3.03 Ah $LiNiCoAlO_2$ NCA cylindrical battery

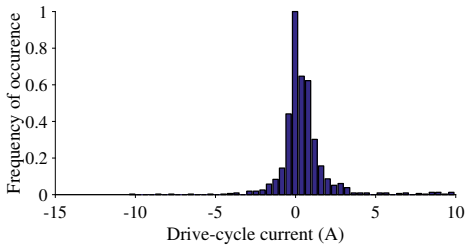

(c) Normalised drive-cycle histogram

Figure 1: Examples of current signals used for an ECM parametrisation and validation. A contrasting difference is seen in amplitude coverage by the two signals. Positive current is assumed to be discharging

or discharge pulse can be used to obtain the corresponding charge/discharge parameters of a Li-ion battery Equivalent Circuit Model (ECM) [1]. In practice however, an ECM based on a single charge and discharge pulse is used to represent the battery dynamics at that particular SoC and battery temperature [2, 3, 4]. In contrast, the work in [5] presents a current dependent ECM whereby the model estimated for all the pulses is included, and therefore the

ECM parameters are a function of current, SoC and battery temperature.

The ECM parameters are usually obtained by minimising the sum of squared errors between the measured and simulated voltage via some non-linear least squares algorithm [6, 7]. By applying the PPC current sequence and measuring the corresponding voltage response (which together forms the estimation data set) at different SoCs and at different battery temperatures, an ECM can be parametrised as a function of SoC and temperature, and if required, be parametrised for charge/discharge and C-rate.

The ECM model is then validated with a drive-cycle current profile (validation data set) which when compared to a pulse current is more dynamic in amplitude (Figure 1) and frequency (as illustrated in Section 2). Figures 1b and 1c show an example of a drive-cycle current profile and its amplitude distribution recorded from a prototype electric vehicle when driving in an urban environment with frequent accelerations and regenerative braking.

As such the PPC current pulses, voltage responses and parametrisation method can be considered sufficient, if upon validation, the model root mean square error (RMSE) and peak error (pk-error) is within an acceptable range. The suitability of the PPC test should however be scrutinised if the assumed ECM structure sufficiently fits the PPC data set during model estimation but still leads to a large RMSE in the validation stage.

An important characteristic of a Li-ion ECM is that it is a data-reliant lumped parameter model. While an ECM attempts to incorporate certain dynamical characteristics of a Li-ion battery the model is not derived from a first principle physics based approach as is done for an electrochemical battery model [8]. The data reliance implies that the suitability of the ECM is

restricted to the domain in which it is parametrised. In this regard the current and voltage data used for model estimation play a crucial role. While SoC and temperature are understood as key operating conditions the characteristic of the current signal is often ignored when parametrising a data-reliant ECM model. An approach to evaluate the validity of a current signal is to compute its frequency spectrum and compare the signal bandwidth to that of the validation current signal. The estimation current signal can then be considered appropriate if its bandwidth spans to include the frequency region of validation.

In this paper a new signal design technique is presented to generate a current signal, defined here as a *pulse-multisine*, which is more dynamic in amplitude and frequency in contrast to a PPC pulse. This signal then provides a better representative estimation data set (in terms of the frequency spectrum) of the expected validation data to subsequently develop a data reliant Li-ion battery model, such as an ECM.

The concept of the pulse-multisine is to excite the battery over a higher frequency range, similar to performing an Electrochemical Impedance Spectroscopy (EIS), while combining the advantage that the signal has sufficient power similar to a PPC signal. This combination of a high frequency range similar to an EIS and high power from a pulse is a compromise and has its limitation. It is a compromise because large current amplitudes (for high power) can cause a battery to behave non-linearly and it is a limitation since to excite a battery over a high frequency range requires a high sampling frequency (at least twice the highest frequency of interest). Any non-linear battery behaviour can be characterised and modelled, as described in Part 2

of this paper series, while the sampling frequency is restricted by the hardware of the laboratory battery cycler.

The pulse-multisine design procedure consists of five tunable parameters enabling the signal to be easily adapted to a given maximum 10 s charge and discharge battery current pulse. The characterisation method based on a pulse-multisine is similar to a PPC in that each pulse-multisine signal is applied at a given SoC and battery temperature. Furthermore, in contrast to a PPC the time for experimentation is in the order of a few minutes instead of several hours. Pulse-multisine signals are therefore both efficient in experimentation time and improves model accuracy as demonstrated in Section 4 and Part 2 [9].

The motivation, signal design methodology and discussions in the paper are detailed as follows: Section 2 explains the potential drawback for using a single pulse for a Li-ion ECM identification. The section also describes how a user-defined base-signal can be combined with a random phase multisine enhancing the base-signal amplitude and bandwidth to generate the pulse-multisine signal. Section 3 gives a set of rules on how the pulse-multisine design parameters can be tuned and an example of its performance is given in Section 4. Section 5 discusses the advantages of the pulse-multisine for experimentation and modelling, and perspectives and conclusions are given in Section 6.

2. Pulse signal limitation and pulse-multisine signal design

A battery is a system governed by differential equations (a dynamic system), this implies that the voltage response at the terminals will depend also

on the frequency content and bandwidth of the excitation current signal, this is a fundamental property of any dynamical system [10]. As such, one way to assess the suitability of a current signal for model estimation is to examine its frequency spectrum. If in comparison, the validation signal spans a higher bandwidth the model will not capture the higher dynamics as it has been estimated over a narrower or different bandwidth. Figure 2 shows the magnitude of the Discrete Fourier Transform (DFT) of the 20 min drive-cycle (shown in Figure 1b) up to 1 Hz, which is used for model validation, and of a 10 s followed by a 30 min rest 2 C mid-pulse from the PPC test procedure, which is used to characterise the NCA 3.03 Ah battery (Figure 1a). A sampling frequency of 10 Hz is used in the DFT calculations to plot the spectra of the drive-cycle and 2 C pulse in Hz. In this paper the DFT of a sampled

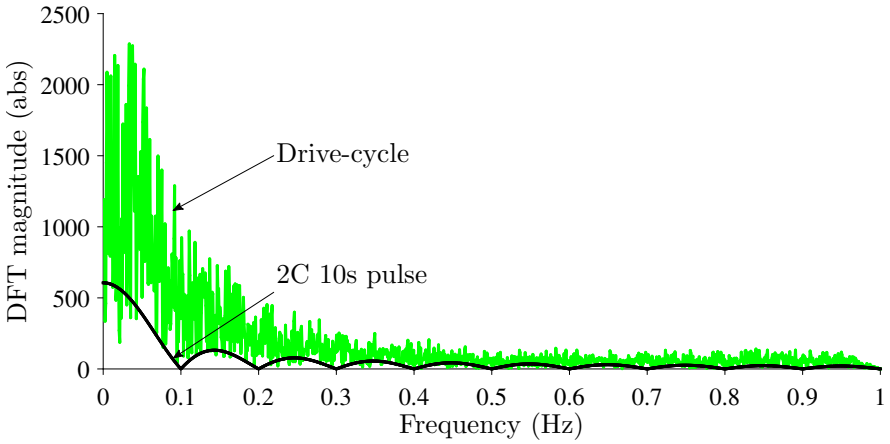

Figure 2: Frequency spectrum of the drive-cycle and a 2 C 10 s pulse

signal $s(n)$ is defined as:

$$S(k) = \sum_{n=0}^{N-1} s(n) e^{-j2\pi kn/N} \quad k = 0, 1 \ldots, N-1 \tag{1}$$

where $S(k)$ is the DFT at harmonic k and N is the total number of samples of the signal $s(n)$. The harmonic number k can then be related to frequency as $f = kf_s/N$ Hz with f_s being the sampling frequency in Hz.

The Fourier transform of a unit magnitude pulse signal of time duration T_p seconds is $T_p\text{sinc}(\pi f T_p)$, where f is the frequency in Hz. For such a signal 90 % of the signal power, in comparison to the total signal power, is within the first lobe ($0 \leq f \leq 1/T_p$ Hz) and the remaining 10% is spread across the frequencies above $1/T_p$ Hz [11].

As such, with a pulse width of $T_p = 10$ s in a PPC signal, 90 % of the pulse energy is focused in the lower frequencies up to $1/T_p = 1/10 = 100$ mHz and all subsequent lobes decrease with frequency (Figure 2). In comparison, the DFT magnitude of the drive-cycle shows that most of its energy is considerably higher in the lower frequencies (up to around 400 mHz-500 mHz) and remains around the same value up to 1Hz.

The low magnitude and frequency coverage of the pulse signal suggests that an ECM model estimated with a pulse can under perform when simulating a drive-cycle scenario. As the pulse signal (estimation data) encompasses a narrower bandwidth than the drive-cycle signal (validation data). A signal with a higher magnitude and frequency coverage is therefore required for a Li-ion ECM model parametrisation. A new signal design methodology is presented in the following sections such that the resulting characterising current signal is sufficiently dynamic in both amplitude and frequency domain. The key idea behind the design methodology is the summation of a low frequency signal component, which is referred to as the *base-signal*, with a high frequency signal realised in the form of a *multisine* signal to generate

a signal termed here as the pulse-multisine with drive-cycle frequency and amplitude characteristics.

2.1. Base-signal design

Prior to parametrising and designing the base-signal it is necessary to know the maximum 10 s discharge (C_{dmax}) and 10 s charge (C_{cmax}) pulses defined by the manufacturer. These values are often available in the battery data-sheet and at times given for a particular SoC and battery temperature. Furthermore, both C_{dmax} and C_{cmax} are assumed to be positive values. The base-signal has four design parameters (α, T_1, T_2 and T_4) and an example for a scenario where $C_{cmax} < C_{dmax}$ is shown in Figure 3a.

The base-signal consists of a discharge and charge pulse and two rest intervals of time T_2 and T_4 seconds (see Figure 3a). The base-signal could also start with the charge pulse followed by the discharge pulse as the sequence order has no significance. The discharge and charge pulse need not be equal in magnitude or time duration and the pulse amplitude will depend on the values of C_{dmax} and C_{cmax}. If for example $C_{cmax} < C_{dmax}$ (as in Figure 3a) the C-rate of the corresponding charge pulse in the base-signal will be lower than the discharge pulse. Similarly, the discharge pulse will be lower if $C_{dmax} < C_{cmax}$. Let the C-rate and time duration of the larger of the two base-signal pulses be defined as C_1 and T_1 seconds respectively and similarly C_2 and T_3 seconds for the smaller pulse.

Given that C_{dmax} and C_{cmax} can be different, depending on the SoC and battery temperature, two new parameters C_{min} and C_{max} are defined as

follows

$$C_{min} = \min\{C_{dmax}, C_{cmax}\} \tag{2}$$

$$C_{max} = \max\{C_{dmax}, C_{cmax}\} \tag{3}$$

The C-rate of the smaller pulse (C_2) in the base-signal is then set equal to a fraction α of C_{min},

$$C_2 = \alpha C_{min} \tag{4}$$

The reason for using a fraction of the maximum allowed C-rate is because the remaining portion ($\beta = (1 - \alpha)$) will be accounted for when superimposing the high frequency multisine whose maximum C-rate will be set to βC_{min} (multisine design is described in Section 2.2)

$$\therefore \beta = 1 - \alpha \tag{5}$$

Similar to α, a parameter γ dictates the C-rate of the larger pulse (C_1) in the base-signal and sets its amplitude to a fraction of C_{max}

$$C_1 = \gamma C_{max} \tag{6}$$

Unlike α, γ is not a design parameter since the multisine signal will at most contribute βC_{min} in magnitude towards C_{max}, to ensure that the base-signal does not exceed C_{max}, γ should therefore fulfil the following constraint

$$\begin{aligned} C_{max} &= \beta C_{min} + \gamma C_{max} \\ \therefore \gamma &= \left(C_{max} - \beta C_{min}\right) / C_{max} \end{aligned} \tag{7}$$

Furthermore, the battery should not undergo a net discharge or charge from the application of the base-signal. This property is similar to a PPC

pulse sequence which ensures that the SoC of battery is the same prior to and post application of the profile. The base-signal is therefore designed to be a zero mean signal when averaged over time (the superimposed multisine will also have a zero mean). This allows one of the pulse time durations to be set freely while constraining the other. Since α is a design parameter which sets the C-rate of the smaller pulse, the time interval T_1 of the larger pulse is now set as the design parameter. Doing so will ensure that neither the charge nor discharge pulse in the base-signal is disproportionately large or small in comparison to each other. As such T_3 is

$$\begin{aligned} C_1T_1 - C_2T_3 &= 0 \\ \therefore T_3 &= C_1T_1/C_2 \quad C_2 > 0 \end{aligned} \tag{8}$$

and $T = T_1 + T_2 + T_3 + T_4$ is the total time duration of the base-signal.

Setting the C-rate of the base-signal pulses via equations (4 and 6) and constraints (5, 7 and 8) will ensure that once the multisine signal (with an amplitude of βC_{min}) is superimposed the resulting signal will at most span the maximum specified discharge and charge C-rates and not exceed these limits. The four design parameters of the base-signal are therefore:

- α: A value between $0 < \alpha < 1$ and dictates the C-rate of the smallest pulse
- T_1: Time duration of the larger pulse in seconds
- T_2: Time duration of the first rest interval in seconds
- T_4: Time duration of the last rest interval in seconds

2.2. Multisine signal design

A multisine signal (equation 9) is a periodic signal (a signal that repeats) composed as a sum of sinusoids and provides flexibility in the design of its amplitude spectrum and harmonic content.

$$u(n) = \sum_{k=1}^{F} A_k \sin(2\pi k n f_s/N + \phi_k) \quad n = 0, \ldots, N-1 \tag{9}$$

In equation (9) A_k is the amplitude and ϕ_k the phase of the k^{th} harmonic, f_s the sampling frequency, N the number of samples per period and F denotes the highest harmonic number of the signal. The period N of a multisine can be freely chosen, which by Shannon sampling theorem then sets an upper bound on the highest possible harmonic to $F \leq N/2$ and the frequency resolution to $f_0 = f_s/N$ Hz. The product Ff_0 sets the bandwidth of the multisine signal and should span the bandwidth of the drive-cycle for battery model estimation. Furthermore, as the DC component ($k = 0$) in equation (9) is omitted, $u(n)$ is a zero mean signal.

When generating a multisine signal, arbitrary harmonics can be suppressed by setting the corresponding amplitude A_k to zero while the remaining excited harmonics are given identical amplitudes. This is then known as a *flat-amplitude spectrum* multisine; the set of excited harmonics is denoted as H_{exc}. For a flat-amplitude spectrum, the harmonic amplitude A_k can be set arbitrarily if the resulting multisine signal is rescaled to take a desired maximum value K. Therefore A_k is set to 1 for all the excited harmonics and the generated multisine is then scaled to the desired maximum value. Let $\tilde{u}(n)$ be the scaled multisine and is related to $u(n)$ as follows:

$$\tilde{u}(n) = K \frac{u(n)}{\|\boldsymbol{u}\|_\infty} \tag{10}$$

In equation (10) K is the desired maximum magnitude of the random-phase multisine signal and $\boldsymbol{u} = [u(0), \ldots, u(N-1)]$.

The choice for the phases ϕ_k influences the crest-factor[1] of the resulting signal. For example, assuming all harmonics up to $F = N/2$ are present, if $\phi_k = -k(k-1)\pi/F$ the resulting signal will have a low (< 2) crest-factor of around 1.7 and the signal is termed as a *Schroeder phase* multisine [12, 13]. The phases can also be numerically optimised to further reduce the crest-factor [14, 15, 16] or optimised such that the time-signal magnitude distribution is either positively or negatively skewed [17].

Another choice for the phases is to sample the phases randomly from a uniform distribution in the interval $(-\pi, \pi)$ radians. The generated signal is then known as a *random-phase* multisine. A useful property of such a signal is that it approaches a normal distribution in magnitude as the number of harmonics increases [18, 19]. This implies that most of the signal samples will occur around the zero mean value and therefore can be used as a current profile for examining the dynamics of a battery around a particular open-circuit-voltage.

An example of a random-phase multisine is shown in Figure 3. A sampling frequency of $f_s = 10$ Hz is assumed, the maximum signal magnitude is set to $K = 5$ and N is set to $N = 600$ giving a signal period of 60 s. The frequency resolution is therefore $f_0 = 1/60$ Hz and, as for the example, only the odd harmonics are excited equally (a flat-amplitude spectrum) up to 1 Hz and all even harmonics are suppressed. The approximate normal distribution of

[1] Crest-factor is the ratio of a signal's absolute maximum and its rms.

the time-signal and flat-amplitude spectrum of the DFT magnitude up to 1 Hz are seen in Figures (3c) and (3d) respectively.

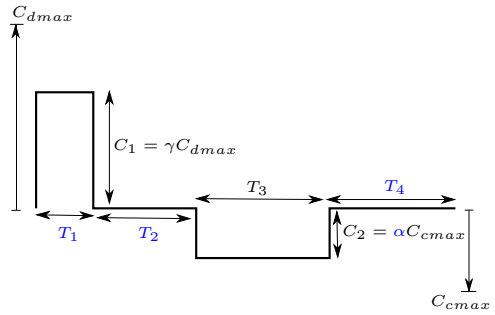

(a) Parametrisation of the base signal, assuming $C_{cmax} < C_{dmax}$, with design parameters α, T_1, T_2 and T_4

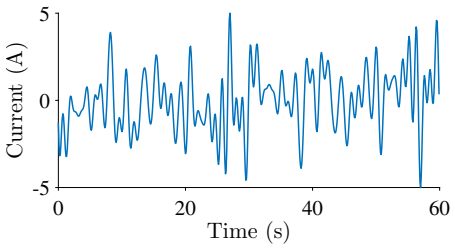

(b) An example of a random-phase multisine, with $f_s = 10$ Hz, $N = 600$, $K = 5$

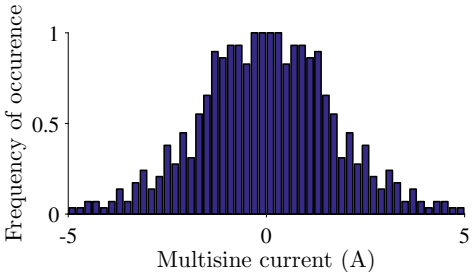

(c) Normalised histogram of multisine approximates a normal distribution

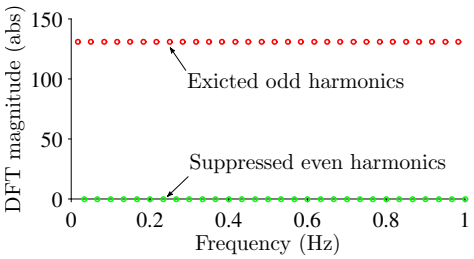

(d) DFT magnitude of multisine showing excited and suppressed harmonics. H_{exc} : all odd harmonics up to 1 Hz.

Figure 3: A base-signal and a random phase multisine

The design parameters of a general flat-amplitude multisine signal are therefore:

- N: The number of samples per period
- K: The maximum magnitude of the random-phase multisine signal

- H_{exc}: Set of excited harmonics

2.3. Pulse-multisine signal

With the design procedures for the base-signal and random-phase multisine in place, the two signals can be superimposed to generate a *pulse-multisine* signal. Though N and K appear as multisine design parameters, these values will be constrained to $N = Tf_s$ and $K = \beta C_{min}$ (as described in Section 2.1) when superimposing the base-signal; therefore the pulse-multisine signal has five design parameters and are:

- α: Which dictates the C-rate of the smallest base-signal pulse, $0 < \alpha < 1$
- T_1: Time duration of the larger base-signal pulse in seconds
- T_2: Time duration of the first rest interval in the base-signal in seconds
- T_4: Time duration of the last rest interval in the base-signal in seconds
- H_{exc}: Set of excited harmonics of the multisine signal

When deciding on the excited harmonic set H_{exc}, the designed base-signal can be used to set the excited harmonic specification. By computing the DFT magnitude of the base-signal, multiples of any suppressed harmonics (where the DFT magnitude is zero) can be identified. For example, the base-signal may have all harmonics excited or multiples of 2 suppressed or other harmonic combinations suppressed. These harmonic multiples can then be suppressed, within the bandwidth of interest, to get H_{exc} for the multisine signal.

Figure 4 shows the superposition of the base-signal and multisine to generate a pulse-multisine signal. The figure illustrates how the amplitudes of the base-signal and multisne combine to span the maximum 10 s discharge (C_{dmax}) and 10 s charge (C_{cmax}) pulses defined by the manufacturer.

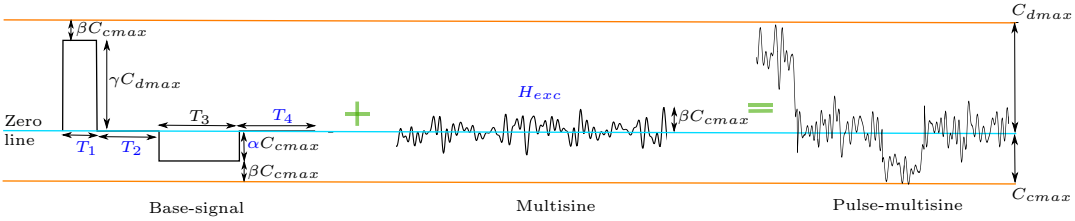

Figure 4: Overall design of a pulse-multisine signal. The superposition of the base-signal and multisine generates a signal dynamic in amplitude spanning the maximum recommended 10 s charge and discharge current

3. Selection of pulse-multisine design parameters

Ideally the five design parameters of the pulse-multisine signal should be related to the battery SoC and temperature. Establishing a direct functional relationship between SoC, battery temperature and the design parameters is difficult and at this stage is unclear. Which necessitates the vales of C_{dmax} and C_{cmax}, from the battery data sheet, as a pre-requisite for the pulse-multisine design. In this paper, however, a set of rules is provided to assist on how the choice of the parameters will influence the pulse-multisine signal design.

The value of α which is between $0 < \alpha < 1$ dictates the amplitude of the smaller base-signal pulse. As its value approaches one β approaches zero ($\beta = 1-\alpha$). Therefore the amplitude of the multisine (βC_{min}) will tend to zero and the pulse-multisine signal will resemble more of the base-signal (see Figure

4). Similarly as α tends to zero the smaller pulse in the base-signal vanishes and to satisfy the zero mean property of the base-signal the larger pulse in the base-signal also vanishes. The pulse-multisine signal therefore resembles more of the random-phase multisine as α tends to zero. As a starting point, a value of $\alpha = 0.6$ is found to offer a good compromise whereby the histogram of the resulting pulse-multisine signal sufficiently spans the maximum and minimum 10 s battery C-rates (C_{dmax} and C_{cmax}) and amplitude spectrum coverage.

The time design parameters T_1, T_2 and T_4 influence the total time duration of the pulse-multisine signal T. A large value for T has the advantage that the frequency resolution improves ($f_0 = 1/T$ Hz) and as f_0 decreases it also gives access to the battery dynamics at a lower frequency. However, the battery temperature may increase considerably (> 10 °C) when applying several periods of a pulse-multisine with a large time period (T). This increase in temperature will then influence the estimation of the corresponding ECM parameters which ideally requires a constant SoC and temperature to avoid parameter variation. Through several experimental runs in the laboratory on a selection of energy and power Li-ion batteries, five periods of a pulse-multisine with a period in the order of a minute resulted in a battery temperature rise of around 4-5 °C . In this regard the values for T_1, T_2 and T_4 can be selected to give a pulse-multisine signal period of approximately $T \approx 60$ s which subsequently gives a fundamental frequency of approximately 17 mHz.

With the design parameter H_{exc}, as described in Section 2.3, the DFT of the base-signal will indicate which harmonics to be excited. However,

the highest harmonic number in H_{exc}, defined as F, is a free parameter but is bounded (through Shannon sampling theorem) by the sampling frequency and fundamental frequency as $F \leq f_s/(2f_0)$. The highest harmonic F should be set such that it sufficiently spans the bandwidth of the drive-cycle. Denoting the highest desired pulse-multisine frequency as f_{max} the highest harmonic is then $F \times f_0 \simeq f_{max}$ Hz and as F is an integer $F = \lfloor f_{max}/f_0 \rfloor \leq f_s/(2f_0)$, where $\lfloor \bullet \rfloor$ is the rounding down operation. Based on the drive-cycle example presented in this paper most of its energy is present up to around 500 mHz and f_{max} is therefore set to 1 Hz. As a starting point a bandwidth of 1 Hz could be used when designing a pulse-multisine signal, if a battery is expected to experience very dynamic signals the value of f_{max} should be increased to capture this bandwidth range.

Therefore as a rule-of-thumb when designing a pulse-multisine, α can be set to 0.6, the time parameters T_1, T_2 and T_4 are set to to give a signal period of approximately $T \approx 60$ s and the maximum harmonic in H_{exc} is set to 1 Hz.

3.1. Two pulse-multisine signal examples

Two pulse-multisine signal examples for the 3.03 Ah NCA battery are presented below based on the manufacturer recommendations for the maximum applicable 10 second currents (C_{dmax} and C_{cmax}) that were provided for a range of SoCs and battery temperatures. Signal 1 is for a case where $C_{dmax} = C_{cmax} = 3.8$ C and due to the equal charge and discharge recommended C-rates it is a signal appropriate for use at mid SoC regions. Signal 2 is for a case where the maximum recommended 10 s discharge current is higher than the maximum 10 s charge current ($C_{dmax} > C_{cmax}$) and is there-

fore a signal appropriate to use when the battery SoC is high (for example when at 80%). The pulse-multisine design parameters for Signals 1 and 2 following the description in Section 3 are given in Table 1.

	Battery specification		Design parameters				
	C_{dmax}	C_{cmax}	T_1	T_2	T_4	α	H_{exc}
Signal 1	3.8 C	3.8 C	10 s	20 s	20 s	0.6	Odd harmonics up to 1Hz
Signal 2	8 C	2 C	5 s	20 s	20 s	0.6	Harmonic multiples of 15 suppressed up to 1 Hz

Table 1: Parameters for two examples of a pulse-multisine design for a 3.03 Ah $LiNiCoAlO_2$ NCA battery

With these settings the constrained parameters γ and T_3 of equations (7) and (8) for Signal 1 evaluate to be $\gamma = 0.6$ and $T_3 = 10$ s and for Signal 2 are $\gamma = 0.9$ and $T_3 = 30$ s. Furthermore, the period length of Signal 1 is $T = 60$ s and of Signal 2 is $T = 75$ s. The fact that the two pulses of the base-signal in Signal 1 are equal in amplitude and duration ($\alpha = \gamma$ and $T_1 = T_3$) makes the base-signal of Signal 1 odd-symmetric[2], and the DFT of such a signal will only have energy at odd-harmonics [10]. As such a random-phase multisine with only odd harmonics from 1/60 Hz to 1 Hz (a flat-amplitude spectrum) is generated and superimposed onto the base-signal of Signal 1.

The asymmetry of the base-signal of Signal 2 has harmonic multiples of 15 suppressed (verified by computing the DFT of the Signal 2 base-signal and checking which, if at any, harmonics are at zero). As such a random-

[2]An odd-symmetric signal is when $s(-n) = -s(n)$, where $s(n)$ denotes the signal at sample n

phase multisine with harmonic multiples of 15 suppressed from 1/75 Hz to 1 Hz (a flat-amplitude spectrum) is generated and superimposed onto the base-signal of Signal 2. For both signals the bandwidth is set to 1 Hz as the drive-cycle excited mostly up to 1 Hz (Figure 2). The two pulse-multisines and the normalised histograms are shown in Figure 5.

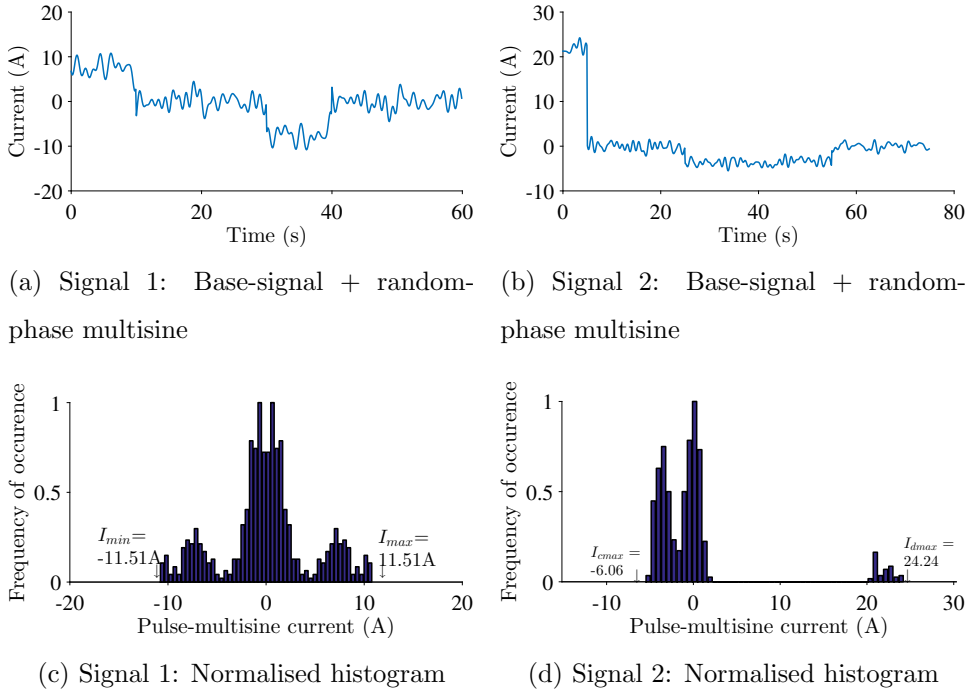

(a) Signal 1: Base-signal + random-phase multisine

(b) Signal 2: Base-signal + random-phase multisine

(c) Signal 1: Normalised histogram

(d) Signal 2: Normalised histogram

Figure 5: Two examples of a pulse-multisine and amplitude distribution. The histograms show better coverage of the applicable maximum to minimum C-rate interval instead of when using a pulse sequence

The superposition of the multisine leads to two main advantages. Firstly, better coverage of the maximum allowed current interval is attained as seen in the histogram of the pulse-multisine signal (Figure 5c and 5d), while only three magnitude values corresponding to C_1, C_2 and zero (as in Figure 3a)

would be achieved had only the base-signal been used. Secondly, the superposition improves the higher frequency signal-to-noise ratio. Referring to Figure 6, which shows the DFT of the base-signal and pulse-multisine for Signal 1, the base-signal contributes mostly to the lower frequencies (< 0.5 Hz) and rapidly decreases above 0.5Hz, by superimposing the flat-spectrum multisine the signal power dose not diminish and improves the signal-to-noise ratio.

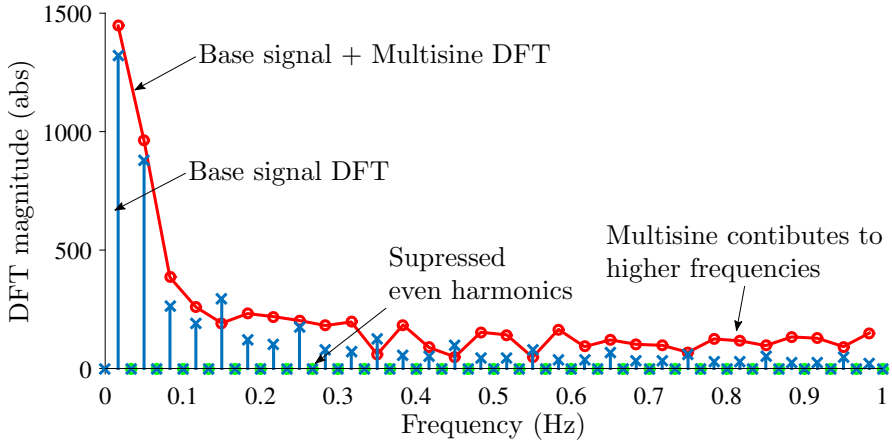

Figure 6: DFT magnitude of the base-signal and pulse-multisine of Signal 1. The addition of multisine enhances the amplitude of the higher (> 0.5 Hz) frequency content had only the base-signal been used. Same conclusion holds for Signal 2

The comparison of the amplitude spectra of the drive-cycle, the 10 s pulse and the two pulse-multisine signals is shown in Figure 7. The amplitude spectrum of the pulse-multisine follows the general drive-cycle spectrum up to 1 Hz. The signal thus captures the characteristic of the drive-cycle allowing the battery to be characterised using a profile similar to which it is validated. The example also illustrates that a pulse-multisine with a representative amplitude spectrum can be designed even when C_{dmax} and C_{cmax} are different.

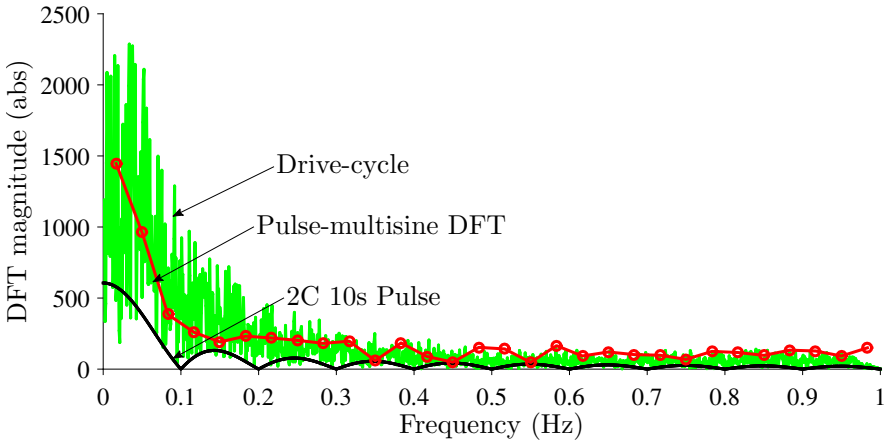

(a) Pulse-multisine Signal 1 spectrum comapred to a drive-cycle and a 2 C 10 s pulse

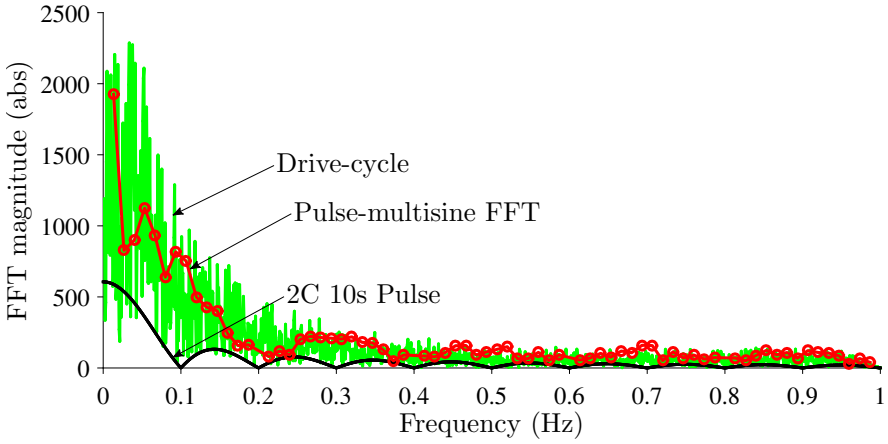

(b) Pulse-multisine Signal 2 spectrum comapred to a drive-cycle and a 2 C 10 s pulse

Figure 7: DFT magnitude comparison of the drive-cycle, a 10 s pulse and pulse-multisine. The magnitude of the pulse-multisine is seen to follow the spectrum of the drive-cycle

4. Pulse-multisine performance

To illustrate that the characteristics (amplitude spectrum and bandwidth) of an estimation data set influence the accuracy of a Li-ion ECM, a model is parametrised with PPC current and pulse-multisine current signals. In [6] a first-order ECM is shown to be sufficient to model pulse responses, as such a first-order ECM is used to model the 18650 3.03 Ah NCA battery.

There is however a minor alteration to the ECM structure based on the estimation data set. The PPC estimation data allows the model parameters to be fitted to a given charge or discharge pulse separately. When fitting the ECM to an individual pulse a temporary series capacitor is included in the model (Figure 8a) to account for the change in SoC (and hence the Open Circuit Voltage (OCV)) prior to and post application of a pulse. The series capacitor is then removed when simulating the model, as the change in OCV will be accounted for by the OCV element in the model. This series capacitor is not required when using the pulse-multisine estimation data (Figure 8b) since the signal is of zero mean and there is no net SoC change. The ECM structure is therefore identical (with C removed) when in simulation during model validation.

The values for C_{dmax} and C_{cmax} were provided by the manufacture over a range of SoCs and temperatures. Following the description in Section 3 different pulse-multisine signals were generated over the different SoCs and temperatures (Table Appendix A.1). The PPC and pulse-multisine signals were then applied over five SoCs (10 %, 20 %, 50 %, 80 % and 95 %) and at four temperatures (0 °C , 10 °C , 25 °C and 45 °C) to parametrise the model.

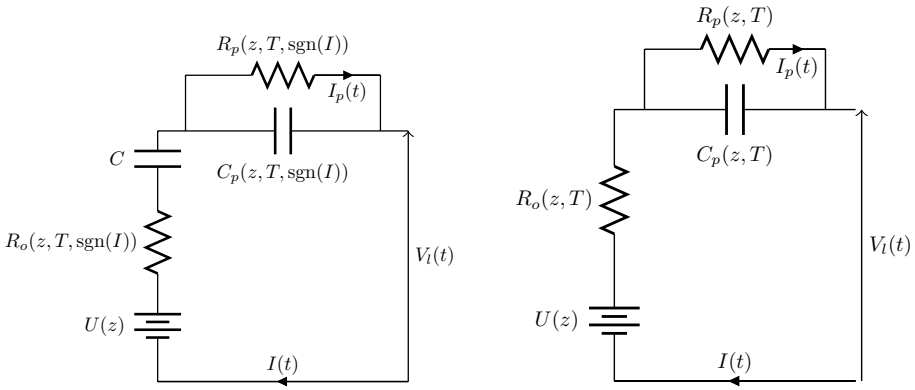

(a) ECM model used with PPC data

(b) ECM model used with pulse-multisine data

Figure 8: The ECM model and its variant during model estimation. The series capacitor (C) in 8a is removed when simulating the model and both model structures are then identical

Once the two estimation data sets (PPC and pulse-multisine) were collected, the model parameters were estimated via a non-linear least squares algorithm (Matlab® `lsqcurfit`) for each SoC and temperature. Furthermore, as PPC data allow model fitting to be done over a charge or discharge pulse, the ECM parameters were also made a function of current sign (charge/discharge) in addition to SoC and temperature. This could improve model accuracy if the battery dynamics differ significantly during discharge or charge. In Figure 8a sgn(I) denote the sign of the current and in Figures 8a and 8b z and T denote SoC and temperature respectively.

The estimated model is then validated with three drive-cycle currents applied at 70 % SoC 10 °C , 70 % SoC 15 °C and 30 % SoC 35 °C . The RMSE and pk-error for the ECM are given in Table 2. The results illustrate

	70 % SoC 10 °C		70 % SoC 15 °C		30 % SoC 35 °C	
	RMSE (V)	Pk-Error (V)	RMSE (V)	Pk-Error (V)	RMSE (V)	PK-Error (V)
ECM (PPC)	3.30 E-02	1.35 E-01	3.20 E-02	1.20 E-01	1.36 E-02	6.74 E-02
ECM (pulse-multisine)	2.82 E-02	7.36 E-02	3.09 E-02	6.74 E-02	1.36 E-02	3.39 E-02
Reduction (%)	14.7 %	45.3 %	3.5 %	43.9 %	0 %	49.7 %

Table 2: RMSE and pk-error of a first-order ECM estimated with PPC and pulse-multisine tests. The use of pulse-multisines and ECM gives consistently reduced RMSE and pk-error for the 18650 Li-ion NCA battery.

that the model estimated based on pulse-multisine compared to PPC data gives consistently improved RMSE and pk-error. The percentage reduction of RMSE and pk-error ranged between 15 % - 0 % and 44 % - 50 % respectively.

This experimental result demonstrates that the amplitude spectrum and bandwidth of the estimation data influences the model accuracy for a given ECM model. Thus by increasing the amplitude spectrum and bandwidth through a pule-multisine the model accuracy can be improved.

5. Discussions

In addition to having a representative spectrum, the pulse-multisine current signal has several other advantages. In the previous section the pulse-mutlsine estimation data were used to parametrise a particular ECM model. However, the signal can be used to improve the model structure of a Li-ion battery ECM. This is achieved by applying several periods of the signal, when at a particular SoC and battery temperature, and driving it to a steady-state behaviour. A non-parametric impedance of the battery is then estimated that

aids in deciding the order and structure the ECM. The amplitude distribution of the pulse-multisines (Figure 5) also allows a non-linear function to be estimated. This function accounts for current dependency of the battery dynamics without having to estimate a separate ECM for charge and discharge dynamics. Details of the new model structure and estimation procedure is given in Part 2 [9].

Depending on the values of C_{dmax} and C_{cmax}, the base-signal of the pulse-multisine may be identical at several SoC and battery temperatures. However, a different realisation of the random phase multisine is then superimposed to the base-signal giving a unique pulse-multisine signal for each of the SoC and battery temperature points of interest. This has the advantage that a voltage response based on a varied set of driving currents is obtained for modelling, rather than using the voltage response to an identical pulse of a PPC test.

If the values of the time parameters in the pulse-multisine (T_1, T_2 and T_4) are tens of seconds a period will generally be in the order of a minute (as the two example signals in Section 3.1). Applying 5-6 periods, will therefore only require around 5-6 minutes in experimentation per SoC and battery temperature. This is a considerable reduction in time when compared to a series of PPC pulses where each pulse is treated as an independent experiment and with a rest of typically 30 minutes between pulses can require approximately 5 hours for experimentation per SoC and temperature (see for example Figure 1a).

Though the pulse-multisine design procedure and spectrum in this paper are based on a particular drive-cycle, the methodology can be adapted to

another profile. This drive-cycle broadly captures bandwidths observed in typical urban driving (differences between urban roads and motorways for example are expected). The procedure will still involve the superposition of a base-signal, which may include several charge and discharge steps and pulse widths, and a random-phase multisine with the appropriate bandwidth matching that of the new drive-cycle.

For any interested person, the design routine to generate a pulse-multisine signal is available to download as a Matlab function from the following Github repository https://github.com/WDWidanage/MatlabFunctions/.

6. Conclusions

The PPC test procedure, though straight forward in design, is limited in bandwidth and amplitude as a signal for Li-ion ECM modelling. With 90 % of the signal power of a 10 s pulse contained up to 100 mHz, a pulse signal insufficiently spans the spectrum when compared to a drive-cycle used for model validation.

By summing a base-signal and a random phase multisine, to form the new signal termed as pulse-multisne, both amplitude and bandwidth can be excited similar to a drive-cycle. The signal is therefore more relevant for model parameter estimation. As a result the validation accuracy of an ECM improved when estimated with pulse-multisine data over PPC data.

The superposition of the low frequency base-signal and high frequency random phase multisine also maintains a generality to design a pulse-multisine for a drive-cycle which may exceed 1 Hz as the drive-cycle example presented in this paper.

The experimentation time, per SoC and battery temperature, when using a pulse-multisine is several minutes and can save considerable time compared to applying a series of 10 s pulses with a 30 minute rest as done for a PPC test.

Acknowledgements

The research presented within this paper is supported by Innovate UK through the WMG centre High Value Manufacturing (HVM) Catapult in collaboration with Jaguar Land Rover and Tata Motors European Technical Centre.

Appendix A. Pulse-multisine design parameter settings for model estimation

	SoC				
	10 %	20 %	50 %	80 %	95 %
C_{dmax}	1	1.2	2	3	2
C_{cmax}	1.2	1.2	2	1.5	0.5
α	0.5	0.6	0.6	0.6	0.5
T_1	5	10	10	10	5
T_2	20	20	20	20	20
T_4	20	20	20	20	20
H_{exc}	1Hz	1Hz	1Hz	1Hz	1Hz

(a) For 0°C

	SoC				
	10 %	20 %	50 %	80 %	95 %
C_{dmax}	1.8	1.8	4	4	2
C_{cmax}	1.8	1.8	3	2	0.5
α	0.6	0.6	0.5	0.5	0.6
T_1	10	10	10	5	5
T_2	20	20	20	20	20
T_4	20	20	20	20	20
H_{exc}	1Hz	1Hz	1Hz	1Hz	1Hz

(b) For 10°C

	SoC				
	10 %	20 %	50 %	80 %	95 %
C_{dmax}	2	3.8	5.6	7	1.2
C_{cmax}	3	3.8	3	6.5	0.5
α	0.6	0.6	0.6	0.6	0.6
T_1	10	10	10	10	10
T_2	20	20	20	20	20
T_4	20	20	20	20	20
H_{exc}	1Hz	1Hz	1Hz	1Hz	1Hz

(c) For 25°C

	SoC				
	10 %	20 %	50 %	80 %	95 %
C_{dmax}	6	6	8	8	4
C_{cmax}	6	6	4	2	1
α	0.6	0.6	0.5	0.6	0.6
T_1	10	10	10	10	10
T_2	20	20	20	20	20
T_4	20	20	20	20	20
H_{exc}	1Hz	1Hz	1Hz	1Hz	1Hz

(d) For 45°C

Table Appendix A.1: Pulse-multisine design parameter values used for the 18650 Li-ion NCA battery model estimation.

References

[1] N. Omar, M. Daowd, O. Hegazy, G. Mulder, J.-M. Timmermans, T. Coosemans, P. Van den Bossche, J. Van Mierlo, Standardization work for bev and hev applications: critical appraisal of recent traction battery documents, Energies 5 (1) (2012) 138–156.

[2] S. Yuan, H. Wu, C. Yin, State of charge estimation using the extended kalman filter for battery management systems based on the arx battery model, Energies 6 (1) (2013) 444–470.

[3] T. Huria, M. Ceraolo, J. Gazzarri, R. Jackey, High fidelity electrical model with thermal dependence for characterization and simulation of high power lithium battery cells, in: Electric Vehicle Conference (IEVC), 2012 IEEE International, IEEE, 2012, pp. 1–8.

[4] C. Birkl, D. Howey, Model identification and parameter estimation for lifepo4 batteries, in: IET Hybrid and Electric Vehicles Conference 2013 (HEVC 2013), London, UK, 2013, pp. 1764–1769.

[5] N. Omar, Ph.D. Thesis: Assessment of Rechargeable Energy Storage Systems for Plug-In Hybrid Electric Vehicles, VUBPRESS Brussels University Press, 2012.

[6] X. Hu, S. Li, H. Peng, A comparative study of equivalent circuit models for li-ion batteries, Journal of Power Sources 198 (2012) 359–367.

[7] G. L. Plett, Extended kalman filtering for battery management systems of LiPB-based HEV battery packs: Part 2. Modeling and identification, Journal of power sources 134 (2) (2004) 262–276.

[8] M. Doyle, Modeling of Galvanostatic Charge and Discharge of the Lithium/Polymer/Insertion Cell, Journal of The Electrochemical Society 140 (6) (1993) 1526. doi:10.1149/1.2221597.

[9] W. Widanage, A. Barai, G. Chouchelamane, K. Uddin, A. McGordon, J. Marco, P. Jennings, Design and use of multisine

signals for Li-ion battery equivalent circuit modelling. Part 2: Model estimation, Journal of Power Sources 324 (-) (2016) 61–69. doi:10.1016/j.jpowsour.2016.05.014.
URL http://dx.doi.org/10.1016/j.jpowsour.2016.05.014http://linkinghub.elsevier.com/retrieve/pii/S037877531630550X

[10] K. Godfrey, Perturbation Signals for System Identification, Prentice Hall, 1993.

[11] H. A. Barker, K. R. Godfrey, System identification with multi-level periodic perturbation signals, Control Engineering Practice 7 (1999) 717–726.

[12] M. R. Schroeder, Synthesis of low peak factor signals and binary sequences with low auto-correlation., IEEE Transactions on Information Theory 16 (1970) 85–89.

[13] R. Pintelon, J. Schoukens, System Identification - A Frequency Domain Approach, John Wiley & Sons, Hoboken, N.J, New York, 2012.

[14] E. Van der Ouderaa, J. Schoukens, J. Renneboog, Peak factor minimisation using a time frequency domain swapping algorithm., IEEE Transactions on Instrumentation and Measurement 37 (1) (1988) 145–147.

[15] E. Van der Ouderaa, J. Schoukens, J. Renneboog, Peak factor minimisation of input and output signals of linear systems., IEEE Transactions on Instrumentation and Measurement 37 (2) (1988) 207–212.

[16] P. Guillaume, J. Schoukens, R. Pintelon, I. Kollár, Crest factor minimisation using non-linear Chebyshev approximation methods., IEEE Transactions on Instrumentation and Measurement 40 (6) (1991) 982–989.

[17] J. Schoukens, T. Dobrowiecki, Design of broadband excitation signals with user imposed power spectrum and amplitude distribution, in: IEEE Instrumentation and Measurement Technology Conference, St. Paul, U.S.A., 1998, pp. 1002–1005.

[18] W. D. Widanage, J. Stoev, J. Schoukens, Design and application of signals for non-linear system identification, in: Proceedings of the 16th IFAC Symposium on System Identification, Brussels, Belgium, 2012, pp. 1605–1610.

[19] R. Pintelon, J. Schoukens, System Identification - A Frequency Domain Approach, IEEE Press, New York, 2001.